EJTAS
ISSN 2786-7447
EUROPEAN JOURNAL OF THEORETICAL AND APPLIED SCIENCES
OPEN ACCESS
PEER REVIEWED

Transition to Turbulence of a Laminar Flow Accelerated to a Statistically Steady Turbulent Flow

Benjamin Segun Oluwadare
Department of Mechanical Engineering, Faculty of Engineering, Ekiti State University, Ado-Ekiti, Nigeria

Paul Chukwulozie Okolie
Department of Mechanical Engineering, Faculty of Engineering, Nnamdi Azikiwe University, Awka, Nigeria

David Ojo Akindele
Department of Mechanical Engineering, Faculty of Engineering, Ekiti State University, Ado-Ekiti, Nigeria

Oluwafemi Festus Olaiyapo
Department of Mathematics, Emory University, Atlanta, United States

Ayobami Phillip Akinsipe
Department of Mechanical Engineering, Faculty of Engineering, Ekiti State University, Ado-Ekiti, Nigeria

Oku Ekpenyong Nyong
Department of Mechanical Engineering, Faculty of Engineering, University of Cross River State, Calabar, Nigeria

Suggested Citation

Oluwadare, B.S., Okolie, P.C., Akindele, D.O., Olaiyapo, O.F., Akinsipe, A.P., & Nyong, O.E. (2024). Transition to Turbulence of a Laminar Flow Accelerated to a Statistically Steady Turbulent Flow. *European Journal of Theoretical and Applied Sciences, 2*(2), 928-943. DOI: 10.59324/ejtas.2024.2(2).82

Abstract:

This current study investigates the turbulence response in a flow accelerated from laminar to a statistically steady turbulent flow utilising Particle Image Velocimetry (PIV) and Constant Temperature Anemometry (CTA). The dimensions of the rectangular flow facility are 8 m in length, 0.35 m in width, and 0.05 m in height. The flow is increased via the pneumatic control valve from a laminar to a statistically steady turbulent flow, and the laminar-turbulent transition is examined. As the flow accelerates to turbulent from laminar, the friction coefficient increases quickly and approaches its maximum value within a short period. As a result, a boundary layer forms extremely near to the wall, increasing the velocity gradient and viscous force. The friction coefficient and viscous force decrease with increasing boundary layer thickness, and transition occurs as a result of instability of the boundary layer. The friction coefficient is used to specify the beginning and end of the transition. The transition starts when the friction coefficient reaches its minimal value. It increases again, and its maximum value marks the end of the transition to turbulence. The study shows that three stages lead to turbulence near the wall when the flow is accelerated from laminar to turbulent. These phases are similar to the transient turbulent flow reported. The reaction of mean velocity as laminar flow is accelerated to turbulent flow is investigated. The mean velocity behaves like a "plug flow" when the flow accelerates from laminar to turbulent, meaning that everywhere in the flow zone, except for the position extremely near the wall, the flow behaves like a solid body. The changes in the channel flow that accelerates from a laminar to a turbulent condition are presented, together with the turbulence statistics, wall shear stress, bulk velocity, and friction coefficient. Like the boundary layer bypass transition and transient turbulent flows, the transition to turbulence follows a similar process.

Keywords: *laminar flow, turbulent flow, constant temperature anemometry, particle image velocimetry, transition, turbulence.*

Introduction

When laminar flow transitions to turbulent flow, it is often due to an increase in velocity or a disturbance in the flow. This transition can occur gradually or suddenly, depending on factors like the Reynolds number, which measures the ratio of inertial forces to viscous forces in the flow. Higher Reynolds numbers typically indicate a transition to turbulence. Factors such as rough surfaces, sharp bends, or sudden expansions in the flow path can also promote turbulence. Understanding this transition is crucial in various engineering applications, such as designing efficient pipes and channels, optimizing airflow over surfaces, and enhancing mixing processes.

One common aspect of accelerating channel and pipe flows is an abrupt change of laminar-turbulent flow. The crucial Reynolds number is where the transition occurred and this is significant for the dynamic control of a channel flow. The transition to turbulence has been primarily studied experimentally and numerically in periodic and non-periodic flows. Although research on accelerating laminar flows has not been reported as much, in recent years a few number of publications have been published in this area. The laminar-turbulent bypass transition serves as the foundation for understanding laminar flow transitioning to turbulent flow. Research on bypass transition is evaluated, since the current study focuses on expanding the previous work. Since Reynolds's initial investigation of the flow (1883), many researchers have been employing computational and experimental approaches to examine the process of laminar-turbulent transition. A thorough understanding of the mechanisms of turbulence is crucial to giving answers for a variety of design problems in engineering, including heat transmission, flow prediction, wall shear stress management, and mixing processes. For instance, linear theory has been used to study flow instabilities that cause turbulence in a pipe or channel when a pressure gradient is applied (Orr, 1907; Schmid, 2001). Meseguer and Trefethen (2003) showed that Reynolds number in a pipe flow would remain stable for extremely minor changes in the flow. It was noted that the flow stayed constant up to $\mathrm{Re_c}(=\frac{U_c\delta}{\nu}=5772.22)$ in Orszag's (1971) study of flat Poiseuille channel flow using the Chebyshev technique. In pipe, channel and boundary layer flows with a significant degree of flow disturbance, the transition might happen early. The crucial Reynolds number in a flow is defined by Schmid (2001) as the Reynolds number at which the flow exhibits linearly unstable.

Burgers (1924) conducted the initial study on laminar-turbulent transition of boundary layer flows, and Dryden (1938; 1939) published the results of extensive investigations on the transition of boundary layer flows on flat plates to turbulence, the transition to turbulence can be divided into two main classes. The first classification of transitions occurs naturally (natural transition), and the transition occurs through a bypass (bypass transition) in the second classification. Viscosity effects make the fluid to move slowly during a natural transition, and the flow is accompanied by mild disruptions. When the flow disturbances increase in size and amplitude, Tollmien-Schlichting (T-S) waves in two dimensions develop, leading to a three-dimensional secondary instability and the eventual breakdown of the turbulent flows. These waves cause turbulence patches in this kind of transition technique, which eventually cause turbulence to begin. Noteworthy, the freestream turbulence in the first classification of transition is much smaller than 0.01 (Tu$\ll$1%). Furthermore, the flow happens at high transitional Reynolds numbers and is characterized by a sluggish process, $\mathrm{Re_x}(=\frac{xU_\infty}{\nu}=10^6)$ (Kleiser & Zang, 1991).

Bypass transition is known as the second transition level and can be determined if the amount of turbulence in the free stream is more than 0.01 (Tu>1%). At a Reynolds number

which is much smaller than 10^6, the breakdown to turbulence may occur. The flow becomes unstable quickly and transitions to turbulence quickly when freestream turbulence is greater than 0.01. In this case, Tollmien-Schlichting waves are avoided in this instance (Morkovin, 1969; Klebanoff, 1971; Saric et al., 2002; Boiko et al., 1994). The term "bypass transition" was first used by Morkovin (1969) in reference to the phenomenon wherein Tollmein-Schlitching waves are bypassed due to substantial amplification of flow disruption.

Tollmien (1929) and Schlichting (1933) were the first to report the solutions for unstable streamwise waves in two dimensions. The Tollmien-Schlichting (T-S) wave name was given to the waves since their presence was confirmed by Schubauer and Skramstad's (1948) experimental study of the zero pressure gradient boundary layer. A rope grid was positioned in the wind tunnel's settling chamber by the authors during the experiment, and the outcomes were compared to the scenario of free stream that was not disrupted. Turbulence patches formed in the flow as a result of an increase in wave activity. Upon reaching turbulent flow that is fully developed, below of the flow boundary layer, there are more turbulence spots covering the whole surface of the wall. After carrying out these experiments, Klebanoff, Tidstrom, and Sargent's (1962) experimental studies demonstrated that, in the case of moderate freestream turbulence, it is independent of Tollmein-Schlichting (T-S) whether high-speed and low-speed streaky structures are amplified in a streamwise direction. Lastly, it has been demonstrated by Morkovin (1984) that when value of freestream turbulence is higher than 0.01 (Tu>1%), the existence of T-S waves has no discernible effect on the transition process. However, it was also reported that as the freestream turbulence is lower than 0.01 (Tu<1%), the amplification of Tollmein-Schlicting (T-S) waves caused the boundary layer transition to occur, according to data from experimental studies on the subject carried out by Roach and Brierley (1992). Tollmein-Schlicting (T-S) waves disappeared when Tu>1%. Consequently, the second transition level, referred to as the bypass transition, generated.

Boiko et al. (1994) showed how the transition process was impacted by Tollmien-Schlichting (T-S) waves when the freestream turbulence value is 15/1000. It was observed that nonlinear/wave interactions involved T-S waves, which led to TS-wave regeneration in the unstable frequency band. Furthermore, in a flow with freestream turbulence larger than 0.01 (Tu>1%), they found difficulty identifying Tollmein-Schlichting (T-S) waves; but, when there is minimal freestream turbulence in the boundary layer of less than 0.01 (Tu<1%), T-S waves were readily identified. When strong freestream turbulence more than 0.01 (Tu>1%) was present in the boundary layer during the tests, the authors inserted regulated oscillations generated through vibrating ribbons for the purpose of identifying small-amplitude waves. They established that it is possible to find small-amplitude waves in a boundary layer when there is at least 0.015 high freestream turbulence. Additionally, the presence of (T-S) waves was shown to enhance the number of turbulence patches that developed and prompted the onset transition.

Three phases of flow development take place during a bypass transition process: the buffeted laminar boundary layer, the intermittent turbulence spot generation zone, and the fully established boundary layer with turbulent flow. A decrease in the friction coefficient and an increase in velocity fluctuations in a streamwise direction are characteristics of the buffeted laminar boundary layer area, where the boundary layer is stable despite instabilities. The disturbances' increasing amplitude causes the streamwise fluctuating velocity to rise. Next, elongated streaks known as Klebanoff modes are formed when low-frequency disturbances break through the boundary layer (Jacobs & Durbin, 2001). Kendall (1985) investigated small spanwise scale elongated forms in a boundary layer flow created by freestream turbulence in a streamwise orientation. Remarkably, at modest levels of freestream turbulence, it is thought that Klebanoff modes contribute to the laminar-to-turbulent transition. Low-frequency oscillations

were seen by the author, and they increased linearly with the flow's boundary layer thickness. For the entirety of the research, the flow maintained a laminar boundary layer flow with very little freestream turbulence (less than 0.05%; Tu < 0.05%) (Watmuff, 2004). Goldstein and Wundrow (1998) and Leib, Wundrow, and Goldstein (1999) conducted comparable research and discovered that both low-speed and high-speed streaky patterns were produced as a result of the flow's low-frequency structures being amplified. It is widely acknowledged that localized disturbances cause the instabilities that eventually transform into turbulence spots in the area where intermittent turbulence spot creation occurs. Additionally, the spots become bigger and merge together in the downstream of the flow. The turbulent boundary layer is formed when the instabilities in the flow are multiplied. By then, turbulence patterns cover the whole boundary layer.

At low Reynolds numbers Re, the motion of a viscous fluid flowing down a smooth surface tends to be regular. The flow in question is referred to as laminar because the viscous force ($\mu u/L$) is greater than the inertial force (ρu^2). Moreover, when the Reynolds number rises, the fluid's flow alters and turns erratic and chaotic. At this point, the fluid's motion becomes complicated and the flow is unstable. The fluid's motion gets more complicated as the velocity increases more. A certain amount of disruption that originates from flow instability is necessary for the flow to turn turbulent. (Taylor, 1923; Davidson, 2015).

Numerous committed researchers in fluid dynamics have conducted experimental and numerical studies on the transition of accelerating flows. They have all significantly advanced the knowledge of the transition in a flow that began at rest and laminar flow accelerated to turbulent flows. The following are their contributions.

A time-delayed laminar-turbulent transition was demonstrated by Leutheusser and Lam's (1977) experimental study of accelerated flow that began at rest. Van der Sande's (1980) research revealed a delay in acceleration when the flow accelerated from rest. At 4.2 s, the crucial Reynolds number $\mathrm{Re_D} = 57500$ in 95% of the final mean bulk velocity— or a mean velocity of 1.15 m/s — the author observed the transition to turbulence. Koppel & Liiv (1977) observed a slowdown in the transition to turbulence from the accelerated laminar flow in their experimental study of an accelerating flow that began at rest. The measurements showed that the acceleration increased from 0.68 to 11.78 m/s^2 and the Reynolds number transitioned from 78,000 to 234500.

Several experimental studies on the laminar-turbulent transition have demonstrated that the crucial Reynolds number occurred in the region between $\mathrm{Re_b}$=1800 and $\mathrm{Re_b}$=2300 (Wygnanski et al., 1975; Wygnanski & Champagne, 1973; Han et al., 2000). Their findings indicate that $\mathrm{Re_b}$=1800 is the minimal Reynolds number at which turbulence will occur from laminar flow. This result is quite similar to what Reynolds' experiment yielded. In subsequent studies Pfenniger (1961), the crucial Reynolds number's value obtained was raised to 10^5.

Also, acceleration of flow from rest conducted by Lefebvre and White (1989) found a much higher crucial Reynolds number. The test segment, measuring $30{,}000\ \mathrm{mm}$ in length and $50\ \mathrm{mm}$ in diameter, was used for the experimental examinations. Throughout the investigation, the values of acceleration ranged 1.8 to 11.8 $\mathrm{m/s^2}$, and it was noted that the global transition happened since it happened nearly simultaneously on every instrument. As the flow's acceleration increased, the beginning of transition increased, with the transitional Reynolds number ranging between 2×10^5 and 5×10^5. Afterwards, in order to increase the understanding of the transition to turbulence, Lefebvre and White (1991) investigated acceleration flow from rest. The diameter of the measuring section was changed by the authors from $50\ \mathrm{m}$ to $90\ \mathrm{m}$. During the study, the acceleration of flow varied between 0.2 to 11.2 $\mathrm{m/s^2}$, and the maximum value of the crucial Reynolds number obtained was $1.1x10^5$. When their test findings were compared to two other factors (the pipe Reynolds number, (Re_D),

and the convective acceleration, (K_a), it became clear that the changeover period depended on both pipe diameter and acceleration. Annus & Koppel (2015) used particle image velocimetry (PIV) to experimentally analyze the transition to turbulence of an accelerating flow that began at rest after their investigation. The authors looked at the velocity component's radial development at the transition point. Consistent with earlier authors' findings, it was determined that pipe diameter significantly affects the Reynolds number at transition. The tests for determining the crucial Reynolds number were carried out earlier by Nakahata et al. (2007) in an accelerated pipe flow. The investigations resembled those carried out by Lefebvre and White (1991), and the Hot-Wire Anemometer's output signal was used to identify the beginning of transition. The crucial Reynolds number equation was then presented by the authors after they studied the correlation that emerged between the two experiments. The authors also confirmed that the diameter and acceleration of the pipe affect the crucial Reynolds number and transition time in an accelerated pipe flow.

Greenblatt and Moss (2003) studied rapid transition in relation to previous work on flow accelerated from rest through experimentation. The time it took to accomplish transition was noted, and they examined the impacts of transition during the flow was decelerated. According to research, the time it took to reach transition rose during an increasing flow and decreased after a flow deceleration.

Kataoka, Kawabata, and Miki (1975) also studied an accelerated flow that began at rest in order to study the transition during the flow acceleration. During the experiment, a solenoid valve and a centrifugal pump were utilized to quickly alter the flow rate. The investigated instances' ultimate flow conditions varied in Reynolds number from $Re = 1910\text{-}11900$. A decrease in the final flow condition was found to shorten the time laminar-turbulent transition. The velocity profiles were measured using the electrochemical method during the experiments, and its development was examined. A minimal profile was noted by the authors close to the axis of the pipe. However, the area halfway between the wall and the centreline showed a maximum velocity profile.

To ascertain the characteristics of turbulence, Kurokawa and Morikawa (1986) conducted theoretical and experimental research on the acceleration and deceleration of transient flows in a smooth pipe. They presented two patterns of the transition process for both slow and fast accelerations during the change from laminar to turbulence. In the event of a rapid acceleration, velocity rose at the transition point in the flow centre but fell near to the wall. Additionally, as the acceleration increased during the laminar-turbulent transition, the authors recorded an increase in Reynolds number at that point. Based on these research results, Lefebvre and White (1989; 1991) conducted experimental studies on the transition in accelerating pipe flow. Using water as the working fluid, the flow began at rest and quickly increased to a statistically stable turbulent flow. It was discovered that the crucial Reynolds number increased with acceleration rate, and the scientists used the collected data to draw a link between acceleration and crucial Reynolds number. More recently, using air as the working fluid, Knisely, Nishihara, and Iguchi (2010) investigated transition in a flow that began from the laminar and maintained at a constant-acceleration.

Usually, an increase in velocity or a disruption in the flow causes laminar flow to turn into turbulent flow. Depending on a variety of variables, including the Reynolds number—a measurement of inertial forces to viscous forces ratio in the flow—this change may occur gradually or suddenly. Turbulence is typically implied by higher Reynolds numbers. Turbulence in the flow route can be caused by abrupt bends, rough surfaces, and fast expansions. Understanding this transition is crucial in several engineering applications, such as constructing efficient pipelines, optimising airflow over surfaces, and improving mixing processes.

Methodology

In this section, the methods for measuring flow velocity and turbulent characteristics during the acceleration to turbulent from laminar are explained. Water is used for all the experiments carried out utilizing the test rig in Figure 1. The length of the channel rig is 8 m while the width and the channel height are 0.35 m and 0.05 m, respectively. Stainless steel adapter, magnetic flow meter, centrifugal pump, honeycomb, pneumatic control valve, open top rectangular tank (bottom tank), overhead tank, and measuring section make up the channel flow facility. A total of 5.31 meters separates the open top rectangular tank from the top tank's water-free surface. At 1.21 meters above the laboratory floor, the channel-test portion is elevated. There is enough space for a continuous flow loop in the open top rectangular tank 's 3000-litre capacity and the above water tank's 1000-litre capacity.

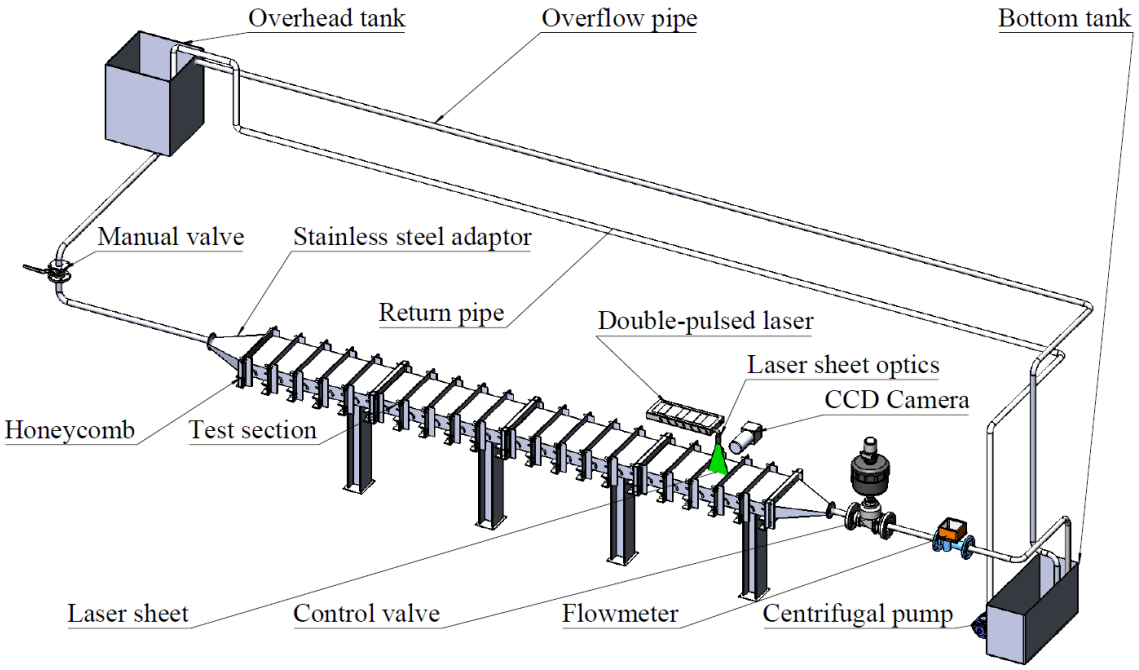

Figure 1. Schematic Diagram of the Flow Facility

Water is moved from the open top rectangular tank to the top tank (overhead tank) using a four-inch PVC transfer conduit and a 2.2 kW, four-inch bore centrifugal pump. A mesh screen was placed over the transfer pipeline end to remove bubbles that were created in the open top rectangular tank due to cavitation and air entrapment. The water in the open top rectangular tank was supplemented with metallic-coated hollow glass spheres that had a mean diameter of 14 µm and a density of 1650 $kg/m3$. A manual valve on the pipeline directs the water from the top water tank into the test portion. A stainless-steel adapter and a flow straightener known as a honeycomb eliminate big whirling flow structures from the inlet of the test channel. Before reaching the open top rectangular tank, the water from the test portion travels via a magnetic flow metre, a pneumatically operated valve, and a stainless-steel valve. Enough water was poured into the pipeline from the magnetic flow metre to keep bubbles from forming in the open top rectangular tank. Transparent Perspex plates were used to construct the test channel. There are four 2000 mm-long chambers in the test portion. The fourth compartment in the test portion housed the measurement apparatus (laser, camera, and hot-film sensors). A glass window was positioned on the side of the fourth

compartment, which is the measuring portion, to enhance optical access. To provide precise flow measurements, the measuring window was positioned 7 m away from the honeycomb. Using a 12-bit Charge-Coupled Device Camera with a resolution of 2048 x 2048 pixels and a frequency of 7 Hz, together with a double-pulse laser (Nd-YAG 65 mJ/pulse) at 400 µs or 600 µs intervals, the Dantec dynamic PIV system was utilized to measure the flow and velocity vectors. We obtained velocity field measurements. The laser used in this study can shoot from the top (vertical-PIV) or from the side (horizontal-PIV) of the test channel. It is possible to measure velocity field in the horizontal and vertical planes using these two mearing methods. In this study, only one orientation was used for the data acquisition. At 7 Hz sample rates, wall shear stress was monitored by the hot-film sensors panel, which was positioned 7.2 m from the test section's entrance. A pneumatic control valve downstream of the test section was quickly opened to provide the necessary accelerating flows. Based on the movement of the seed particle and the pulse time difference, Dantec's dynamic software computes the velocity field. Particle groups are obtained by dividing images from both frames into regions under questioning. In frame one, the particles of each questioning region are clearly marked. It should be possible to link the distinct imprint found in frame one to the questioning region in picture two. Every location in the questioning area has a cross-correlation calculated for it. Frame two yielded the strongest cross-correlation when the imprint was identified. The imprint in the interrogation region of frame two is offset on frame one in order to provide the necessary displacement vector. Once the displacement value was determined, the velocity was calculated by the division of the displacement by the interval between the two pulses. This process was then carried out for each of the remaining interrogation zones.

Data Processing

Spatial, temporal and ensemble averaging were applied to the acquired data using PIV and CTA methodologies in order to compute mean velocity and turbulence statistics. Raw pictures were captured and processed during vertical-PIV measurements using the DynamicStudio program. The acquired data were processed and stored as comma separated values in the software. MATLAB codes were utilised to compute the averages and their derivatives from the acquired data. The anemometer output voltage was recorded using LABVIEW application (ver.18.0) and a National Instruments DAQ card. An ensemble and streamwise spatial average of eighty repeated iterations yielded the statistical quantities of unstable data. Following are the formulas used to determine streamwise mean velocity,

mean square fluctuating velocities, Reynolds shear stress, and unstable wall shear stress.

Unsteady shear stress in the wall is obtained by:

$$\bar{\phi}(t) = \frac{1}{K}\sum_{j=1}^{K} \phi(j,t) \qquad (1)$$

where K is the number of time instants in the determination of temporal average (steady flow) or the number of realizations utilized to execute ensemble-averaged. The j^{th} measurement campaign is denoted by "j". The sample point in time is denoted by "t".

Velocities obtained from ensemble averaged are calculated as follows:

$$U(p,t) = \frac{1}{KN}\sum_{l=1}^{K}\sum_{i=1}^{N}[u(i,l,p,t)] \qquad (2)$$

$$V(p,t) = \frac{1}{KN}\sum_{l=1}^{K}\sum_{i=1}^{N}[v(i,l,p,t)] \qquad (3)$$

Root mean square fluctuating velocities are calculated as follows:

$$u'_{rms}(p,t) = \sqrt{\frac{1}{KN}\sum_{l=1}^{K}\sum_{i=1}^{N}[u(i,l,p,t) - U(p,t)]^2} \quad (4)$$

$$v'_{rms}(p,t) = \sqrt{\frac{1}{KN}\sum_{l=1}^{K}\sum_{i=1}^{N}[v(i,l,p,t) - V(p,t)]^2} \quad (5)$$

Reynolds shear stress is given by:

$$u'v'(p,t) = \frac{1}{KN}\sum_{l=1}^{K}\sum_{i=1}^{N}[u(i,l,p,t) - U(p,t)].[v(i,l,p,t) - V(p,t)] \quad (6)$$

where "l" is the location in the X-direction and K is the total number in this direction; "p" is the location in the wall normal (y) direction; "t" is the time in the transient flow measured from the point when the flow begins to respond to the opening of the control valve; and "i" is the i^{th} realization of the measurement campaign and N is the total number of realizations.

Results and Discussion

Response of Average Velocity, Friction Coefficient and Wall Shear Stress for Laminar Flow Cases

Table 1. Initial Reynolds Number, Final Reynolds Number, Onset Time and Final Time of the Accelerating Laminar Flow

Case	Re_0	Re_1	t_{cr} (s)	t_{turb}(s)
L1	1600	7500	5.67	11.20
L2	1600	9500	4.21	9.22
L3	1600	15600	3.10	5.09

Table 1 shows the data obtained during the accelerating laminar flow to turbulent flow. Figures 1a, 2a and 3a show the variation of bulk velocities of laminar flow cases (L1-3) with a fixed initial Reynolds number, Re_0 =1600 accelerated to final fixed turbulent flow with final fixed Reynolds numbers, Re_0 = 7500, 9500 and 15600, respectively. As the pneumatic control valve is opened, the variation of bulk velocity for each case is obtained. 80 repeated runs are obtained on each case and ensemble average is performed in order to calculate the development bulk velocities, root mean square fluctuating velocities, friction coefficient and wall shear stresses for all the cases investigated. The CCD camera used to capture the velocity field is set to 7 Hz while the time between the two pulses of the laser is set to 600μs.

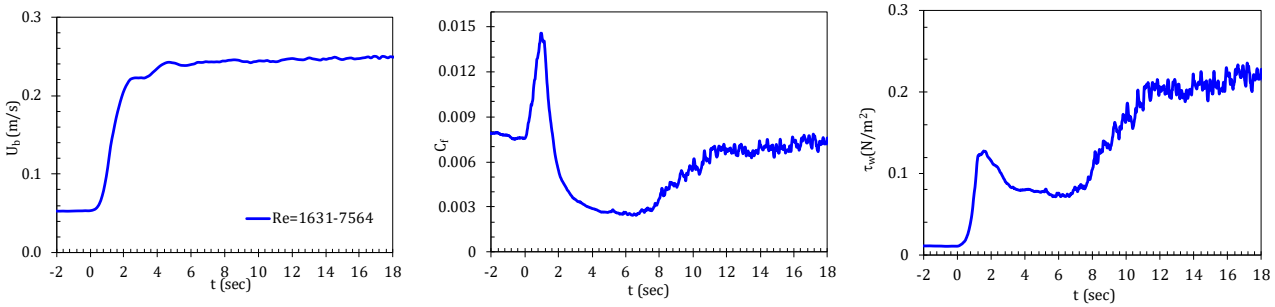

a) b) c)

Figure 1. Development of a) average velocity (U_b), b) friction coefficient (C_f) and c) wall shear stress (τ_w) for laminar case (Re_b=1631-7564)

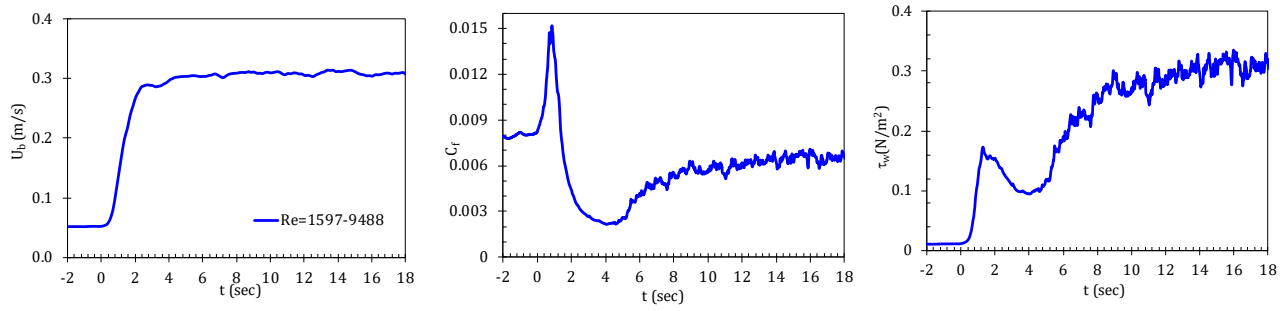

Figure 2. Development of a) average velocity (U_b), b) friction coefficient (C_f) and c) wall shear stress (τ_w) for laminar case (Re_b=1507-9488)

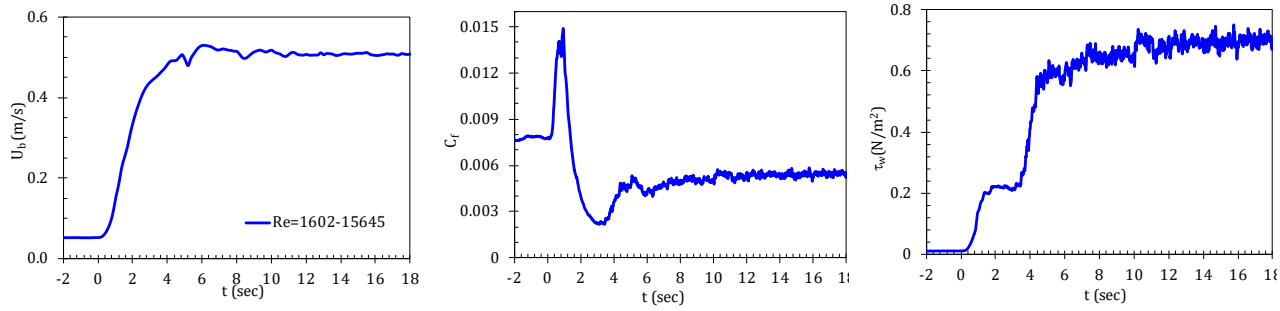

Figure 3. Development of a) average velocity (U_b), b) friction coefficient (C_f) and c) wall shear stress (τ_w) for laminar case (Re_b=1602-15645)

Figures 1(b-c), 2(b-c) and 3(b-c) show the development friction coefficient and wall shear stress for all the laminar flow cases studied. The friction coefficient increases sharply immediately when the accelerating flow started and it reaches the maximum values in minority fraction of a second. This sudden rise causes a thin boundary layer to form very near the wall thereby increases the velocity gradient and viscous force. During the pretransitional period, the boundary layer in the flow grows and causes the friction coefficient to decreases to the minimum values for all the laminar-turbulent cases as shown in Figures 1b, 2b and 3b. Equation 7 is used to determine the friction coefficient's minimal value, which indicates the start of the turbulence transition:

$$C_f(t) = \frac{2\tau_w(t)}{\rho(U_b(t))^2} \qquad (7)$$

As the new turbulence structure is created at the beginning of the transition, it causes the friction coefficient to increase again and attains the maximum value before it becomes statistically steady. The maximum value of the friction coefficient marks the end of transition to turbulence. The transition of accelerating laminar flow to turbulent flow follows the same procedure of the transition of transient channel flow earlier reported by Oluwadare and He (2023), Mathur et al. (2018) and He and Seddighi (2015) and the procedure resembles that of laminar-turbulent transition. Three stages of flow development are also recorded.

Figures 1c, 2c, and 3c show the wall shear stress responses for three cases of flow acceleration from laminar to turbulent. When the laminar flow is accelerated to turbulent flow, a thin boundary layer with high velocity gradient is formed very closed to the wall and this makes the wall shear stress to increase sharply. There is a reduction in the thin boundary layer as it flows into the flow and leads to reduction in the velocity gradient and thereby reduces the wall share stress as shown in Figures 1c, 2c and 3c. During this period, the mean flow continues to accelerate and results in generation of additional boundary layer that spread into the flow. Due to the creation of a temporally growing boundary layer, which causes changes in the flow's structure, the wall shear stress rises again. The development of the wall shear stress of L1, L2 and L3 cases similar to that of faster cases D1-D3 of Oluwadare and He (2023). It is shown that as the final flow condition increases, the shape of the wall shear stress changes and form a four-stage development.

Response of Mean Velocity, Fluctuating Velocity, Wall-Normal Fluctuating Velocity and Reynolds Shear Stress for Laminar Flow Cases

For the laminar flow instances in Table 1, the ensemble average is applied to the 80 repeated runs in order to get the mean velocity, fluctuation and wall-normal velocities, and Reynolds shear stress. The development of the laminar flow accelerated to turbulent flow is studied at the wall locations of $^{y}/_{\delta} = 0.07, 0.2, .045$ and 1. It is revealed immediately following the start of the acceleration of laminar flow to turbulent flow that streamwise mean velocity responds like a "plug flow" at every location except the location of y=1.75 mm from the wall. The weak response at the location of y=1.75 mm from the wall is being that the initial Reynolds number is laminar, as shown in Figure 4a for the case $(Re_b = 1631 - 7564)$, Figure 5a for the case $(Re_b = 1597 - 9188)$ and Figure 6a for the case $(Re_b = 1602 - 75645)$. The bulk Reynolds number is calculated as $Re_b \left(= \frac{\delta U_b}{V}\right)$, where $\delta = h$ is the channel half height, U_b is the bulk velocity of the channel flow and v is the kinematic viscosity of water. Figures 4b, 5b, and 6b illustrates how the mean velocity in the viscous layer responds suddenly during the pretransitional phase at every site with the exception of the center (y=25 mm), when delay occurs. In the flow, the streaky formations elongate and stretch as a result of a sudden rise in the mean velocity near the wall. The increased and extended streaky formations in the flow first appear relatively near to the wall before spreading to the flow's center, as shown by the changing velocity increment. As previously reported by Oluwadare and He (2023), during the pretransitional period of transient turbulent flow, wall-normal and Reynolds stress remained unchanged at every location. In this current study, the Reynolds shear stress and wall-normal fluctuating velocity remain the same during the pretransitional period, as revealed in Figures 4 (c &d), 5 (c & d) and 6 (c & d). This confirms that no turbulence generation during the transitional period.

Based on the lowest value of the friction coefficient, Table 1 shows the transition's start. The Reynolds shear stress and wall normal-fluctuating velocity begin to react at every position, with the exception of the center, as seen in Figures 4 (c & d), 5 (c & d), and 6 (c & d). In the accelerating flow, turbulence is generated as indicated by the reaction of both Reynolds shear stress and wall-normal fluctuating velocity. When both values begin to respond, turbulence is about to begin, and this is the same moment as when the friction coefficient is at its minimum. The laminar starting flow and the pulsating nature of the used laser are the causes of the small discrepancy. The fluctuating velocity rises, overshoots its maximum value, and then falls to a statistically stable value during the transitional phase. The decrease in velocity that is seen extremely near the wall indicates that the streaky structures are breaking down, turbulence zones are forming, and the flow is fully turbulent.

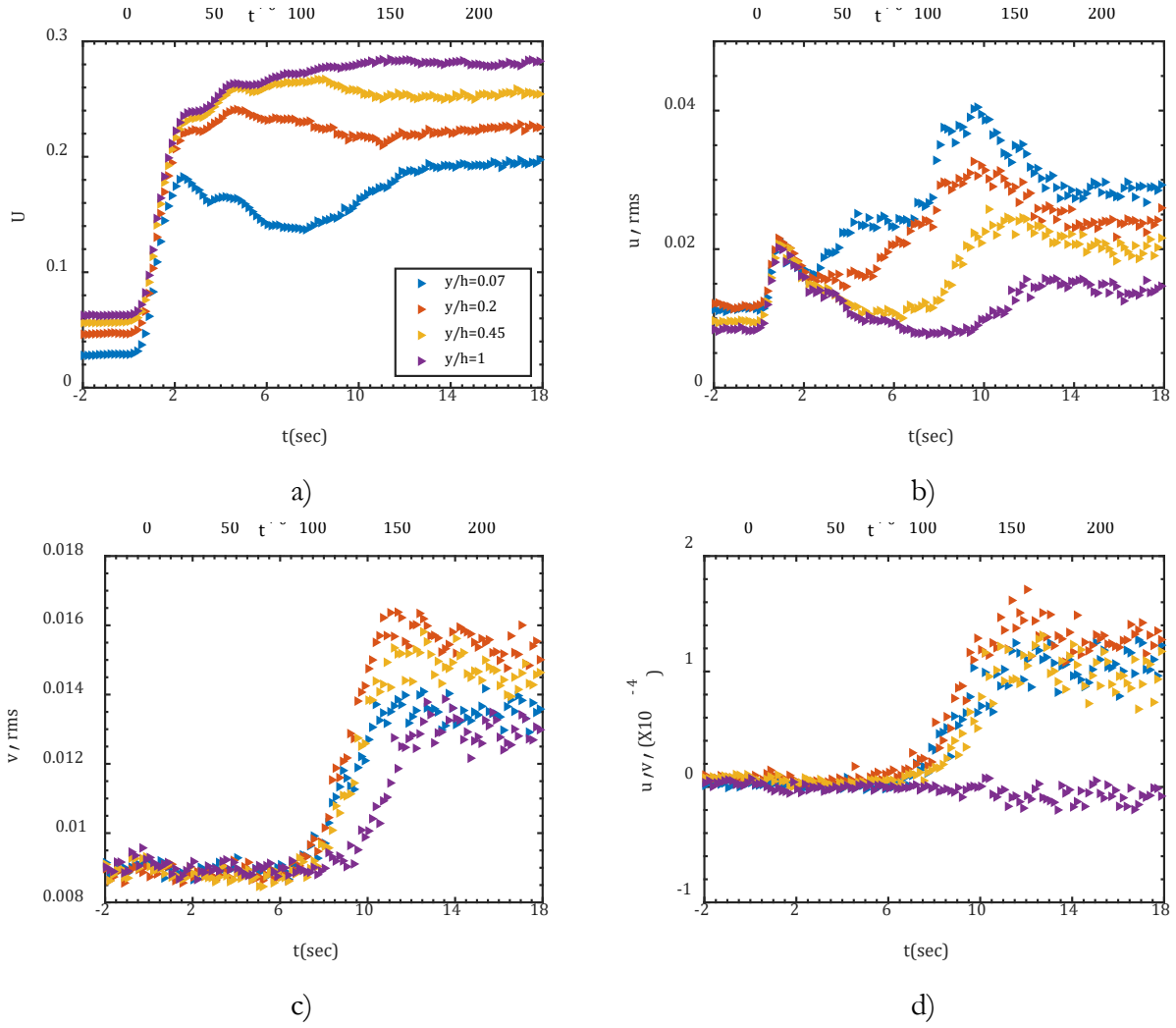

Figure 4. Response of average velocity, fluctuating velocity, wall-normal fluctuating velocity and Reynolds shear stress for Re_b=1631-7564. The four subplots have the same legend, and no normalization is applied to any of the quantities. The unit of subplots (a)-(c) is m/s, while the unit of subplot (d) is m^2/s^2

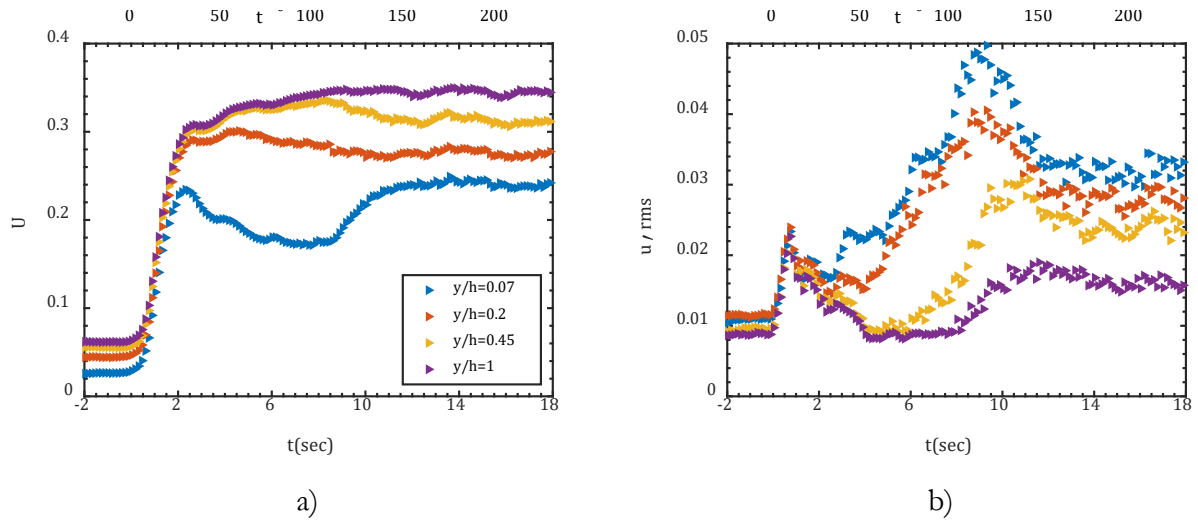

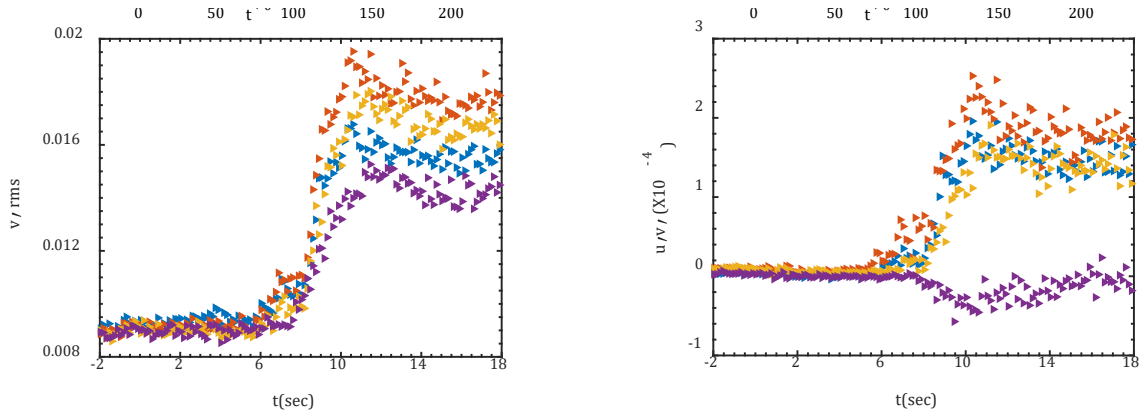

c) d)

Figure 5. Response of average velocity, fluctuating velocity, wall-normal fluctuating velocity and Reynolds shear stress for Re_b=1597-9488. The four subplots have the same legend, and no normalization is applied to any of the quantities. The unit of subplots (a)-(c) is m/s, while the unit of subplot (d) is m^2/s^2

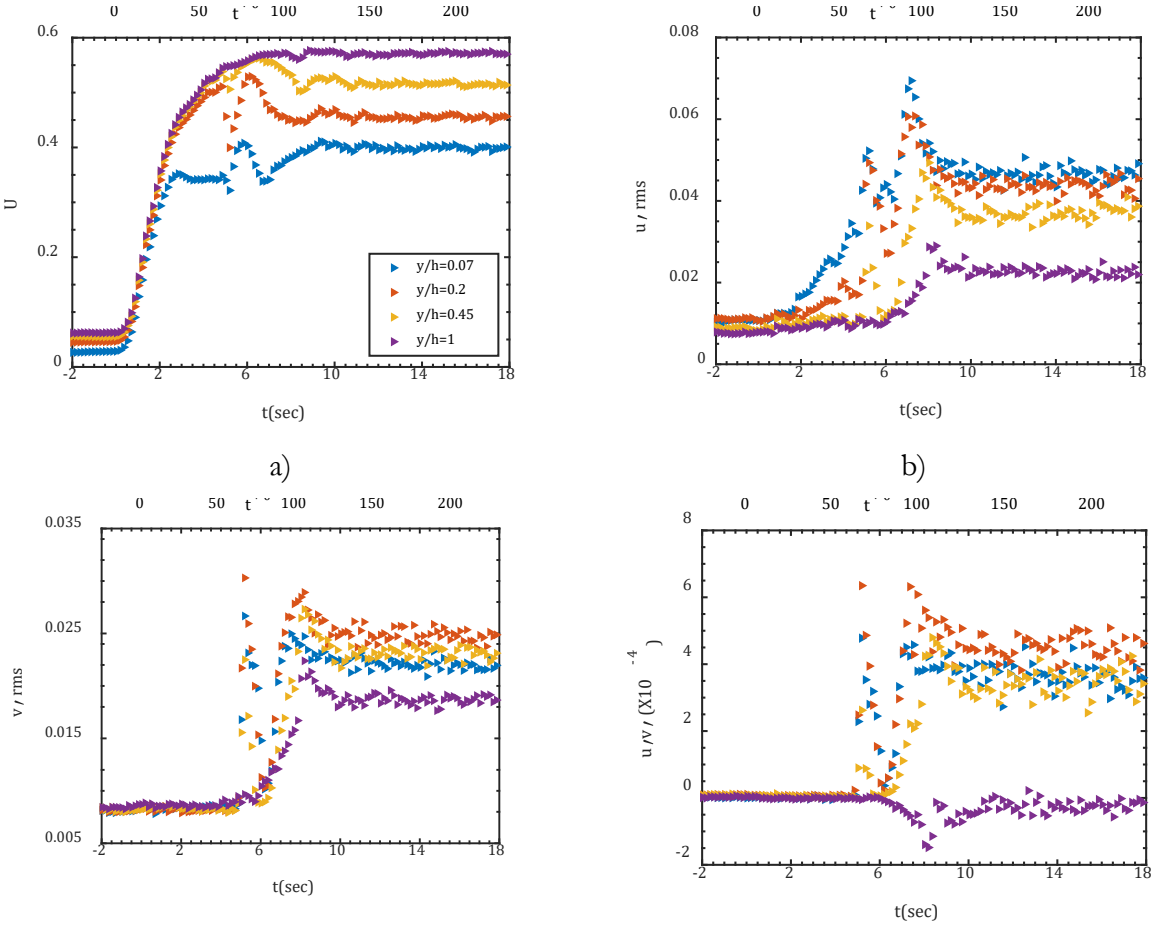

a) b)

c) d)

Figure 6. Response of average velocity, fluctuating velocity, wall-normal fluctuating velocity and Reynolds shear stress for Re_b=1602-15645. The four subplots have the same legend, and no normalization is applied to any of the quantities. The unit of subplots (a)-(c) is m/s, while the unit of subplot (d) is m^2/s^2

Comparison of Friction Coefficient Responses in Laminar-Turbulent Flow

The developments of friction coefficient for all the laminar-turbulent cases accelerated to turbulent flows are compared. The flow is increased from a fixed initial flow condition ($Re_0 = 1600$) to final flow conditions as shown in Table 1. The period of acceleration (a_p) is calculated as the time spent for the initial mean velocity (U_{b0}) to obtain 90% of the final mean velocity (U_{b1}). The acceleration rate (a_r) is obtained as $\frac{(90\%(U_{b1})-U_{b0})}{a_p}$. As the final flow condition increases, the rate of acceleration increases and the beginning of transition decreases, as shown in Figure 7. The process of transient turbulent flow transition of previous studies of He and Seddighi (2013), Seddighi et al. (2014), He and Seddighi (2015) and Oluwadare and He (2023) resembles that of a laminar-turbulent transition due to freestream turbulence despite the initial flow condition is turbulent. The present study exhibits a similar trend in its transition to turbulence, and the friction coefficient development for each case reveals three stages of this transition, resembling the boundary layer flow transition described by Jacobs and Durbin (2001).

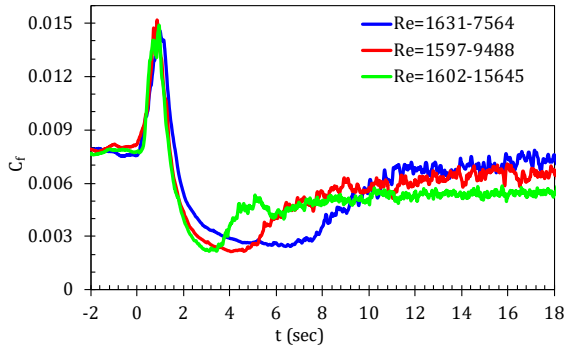

Figure 7. Response of Friction Coefficient (C_f) for the Three Laminar-Turbulent Cases (Re_b=1631-7564, Re_b=1597-9488, Re_b=1602-15645)

Conclusion

Laminar-turbulent channel flow transition has been investigated. It has been demonstrated that, even though the initial flow is laminar, the transition of laminar flow accelerated to statistically steady turbulent flow resembles the laminar-turbulent transition induced by freestream turbulence and the transition of transient turbulent flow. Similar to the spatially evolving boundary layer flow, all the examined laminar-turbulent cases investigated exhibit three steps of the transition to turbulence. These three steps are pre-transition, transition and total turbulent. The friction coefficient trend in this laminar-turbulent channel flow is comparable to the previously investigated transient turbulent flow, both experimentally and numerically. As the final flow condition rises, it is shown that for the cases under study, the beginning of the transition decreases. Moreover, the responses of the turbulence statistics and the mean velocity are examined. According to the study, the mean velocity behaves like a "plug flow" at all locations except y=1.75 mm from the wall as soon as the acceleration of laminar-turbulent flow begins. The initial Reynolds number is laminar, which responsibles for the modest reaction at y=1.75 mm from the wall. Except for the centre (y=25 mm), where there is a delay, fluctuating velocity responds abruptly at every location while the wall-normal fluctuation velocity and Reynolds shear stress stay constant. The fluctuating velocity responds suddenly in the viscous layer during the pretransitional phase. The transition of the laminar-turbulent flow to turbulence begins as both wall-normal fluctuating velocity and Reynolds shear stress begin to increase.

References

Annus, I., & Koppel, T. (2011). Transition to Turbulence in Accelerating Pipe Flow. *Journal of Fluids Engineering, 133*(7), 071202. https://doi.org/10.1115/1.4004365

Annus, I., & Koppel, T. (2015). Development of radial velocity component in accelerating start-

up pipe flow. *European Journal of Mechanics / B Fluids*, *53*, 48–54. https://doi.org/10.1016/j.euromechflu.2015.04.001

Boiko, A., Westin, K., Klingmann, B., Kozlov, V., & Alfredsson, P. (1994). Experiments in a boundary-layer subjected to free-stream turbulence .2. The role of TS waves in the transition process. *Journal of Fluid Mechanics*, *281*, 219–245. https://doi.org/10.1017/S0022112094003095

Burgers, J. M. (1924). The motion of a fluid in the boundary layer along a plain smooth surface. In *Proceedings of the First International Congress for Applied Mechanics, Delft* (pp. 113–128).

Carstens, M. R. (1956). Transition from Laminar to Turbulent Flow during Unsteady Flow in a Smooth Pipe. In *Proc., Int. Congress of Applied Mechanics.* (Vol. 3, pp. 370-377).

Darbyshire, A. G., & Mullin, T. (1995). Transition to turbulence in constant-mass-flux pipe flow. *Journal of Fluid Mechanics*, *289*, 83–114.

Davidson, P. A. (2015). *Turbulence : An introduction for scientists and engineers* (Second edi). Oxford, UK: Oxford, UK.

Dryden, H. L. (1938). Turbulence investigations at the National Bureau of Standards. In *Proc. Fifth Intern. Congress of Appl. Mechanics* (p. 362).

Goldstein, M. E., & Wundrow, D. W. (1998). On the Environmental Realizability of Algebraically Growing Disturbances and Their Relation to Klebanoff Modes. *Theoretical and Computational Fluid Dynamics*, *10*(1), 171–186. https://doi.org/10.1007/s001620050057

Greenblatt, D., & Moss, E. (2003). Rapid transition to turbulence in pipe flows accelerated from rest. *Journal of Fluids Engineering (Transactions of the ASME)*, *125*(6), 1072–1075. https://doi.org/10.1115/1.1624423

He, S., & Seddighi, M. (2013). Turbulence in transient channel flow. *Journal of Fluid Mechanics*, *715*, 60–102. https://doi.org/10.1017/jfm.2012.498

He, S., & Seddighi, M. (2015). Transition of transient channel flow after a change in Reynolds number. *Journal of Fluid Mechanics*, *764*, 395–427. https://doi.org/10.1017/jfm.2014.698

Jacobs, R. G., & Durbin, P. A. (2001). Simulations of bypass transition. *Journal of Fluid Mechanics*, *428*, 185–212. https://doi.org/10.1017/S0022112000002469

Kachanov, Y. S. (1994). Physical Mechanisms of Laminar-Boundary-Layer Transition. *Annual Review of Fluid Mechanics*, *26*(1), 411–482. https://doi.org/10.1146/annurev.fl.26.010194.002211

Kataoka, K., Kawabata, T., & Miki, K. (1975). The start-up response of pipe flow to a step change in flow rate. *Journal of Chemical Engineering of Japan*. Tokyo. https://doi.org/10.1252/jcej.8.266

Kendall, J. M. (1985). Experimental study of disturbances produced in a pre-transitional laminar boundary layer by weak freestream turbulence. In *AIAA Paper*.

Kenneth, B., Takeo, K. (1993). Bypass transition in two- and three-dimensional boundary layers. In *23rd Fluid Dynamics, Plasmadynamics, and Lasers Conference. Fluid Dynamics and Colocated Conferences. American Institute of Aeronautics and Astronautics (1993).*

Klebanoff, P. S., Tidstrom, K. D., & Sargent, L. M. (1962). The three-dimensional nature of boundary-layer instability. *Journal of Fluid Mechanics*, *12*(1), 1–34. https://doi.org/10.1017/S0022112062000014

Kleiser, L., & Zang, T. A. (1991). Numerical Simulation of Transition in Wall-Bounded Shear Flows. *Journal of Fluid Mechanics, 23*(1), 495–537. https://doi.org/10.1146/annurev.fl.23.010191.002431

Knisely, C., Nishihara, K., & Iguchi, M. (2010). Critical Reynolds Number in Constant-Acceleration Pipe Flow From an Initial Steady Laminar State. *Journal of Fluids Engineering (Transactions of the ASME)*, *132*(9), 091202(4)-091202(4). https://doi.org/10.1115/1.4002358.

Koppel', T., & Liiv, U. (1977). Experimental investigation of the development of motion of

liquid in conduits. *Fluid Dynamics*, *12*(6), 881–887. https://doi.org/10.1007/BF01090323

Kurokawa, J. and Morikawa, M. (1986). Accelerated and decelerated flows in a circular pipe. *Bulletin of JSME*, *29*, 758–765.

Lefebvre, P. J., & White, F. M. (1989). Experiments on transition to turbulence in a constant-acceleration pipe flow. *Journal of Fluids Engineering, Transactions of the ASME*, *111*(4), 428–432. https://doi.org/10.1115/1.3243663

Lefebvre, P. J., & White, F. M. (1991). Further experiments on transition to turbulence in constant-acceleration pipe flow. *Journal of Fluids Engineering, Transactions of the ASME*, *113*(2), 223–227. https://doi.org/10.1115/1.2909484

Leib, S. J., Wundrow, D., & Goldstein, M. E. (1999). Effect of free-stream turbulence and other vortical disturbances on a laminar boundary layer. *Journal of Fluid Mechanics*, *380*, 169–203.

Leutheusser, H. J., and Lam, K. W. (1977). Flow Instability in Accelerated Fluid Motion. In *Sixth Can. Congr. App. Mech.,* (pp. 679–680).

Maruyama, T., Kato, Y., & Mizushina, T. (1978). TRANSITION TO TURBULENCE IN STARTING PIPE FLOWS. *Journal of Chemical Engineering of Japan*, *11*(5), 346. https://doi.org/10.1252/jcej.11.346

Maruyama, T., Kuribayashi, T., & Mizushina, T. (1976). THE STRUCTURE OF THE TURBULENCE IN TRANSIENT PIPE FLOWS. *Journal of Chemical Engineering of Japan*, *9*(6), 431. https://doi.org/10.1252/jcej.9.431

Mathur, A., Gorji, S., He, S., Seddighi, M., Vardy, A. E., O'Donoghue, T., & Pokrajac, D. (2018). Temporal acceleration of a turbulent channel flow. *Journal of Fluid Mechanics*, *835*, 471–490. https://doi.org/10.1017/jfm.2017.753

Meseguer, Á., & Trefethen, L. N. (2003). Linearized pipe flow to Reynolds number 10 7. *Journal of Computational Physics*, *186*(1), 178–197. https://doi.org/10.1016/S0021-9991(03)00029-9

Morkovin, M. V. (1984). Bypass transition to turbulence and research desiderata. In Transition in Turbines. *NASA Conf Publ.*, *2386*, pp.161-204.

Morkovin, Mark V. (1969). On the Many Faces of Transition BT - Viscous Drag Reduction. In C. S. Wells (Ed.) (pp. 1–31). Boston, MA: Springer US.

Nakahata, Y., Knisely, C. W., Nishihara, K. Sasaki, Y., Iguchi, M. (2007). Critical Reynolds number in constant-accelerated pipe flow. *J. of the Japanese Society for Experimental Mechanics.*, *7*(2), 142–147.

Oluwadare, B. S.,, & He, S. (2023). Experimental study of turbulence response in a slowly accelerating turbulent channel flow. *Journal of Fluids Engineering (Transactions of the ASME)*, *145*(1), 081202. https://doi.org/10.1115/1.4062166

Orr, W. M. (1907). The Stability or Instability of the Steady Motions of a Perfect Liquid and of a Viscous Liquid. Part I: A Perfect Liquid. *Proceedings of the Royal Irish Academy. Section A: Mathematical and Physical Sciences*, *27*, 9–68.

Orszag, S. A. (1971). Accurate solution of the Orr–Sommerfeld stability equation. *Journal of Fluid Mechanics*, *50*(4), 689–703. https://doi.org/10.1017/S0022112071002842

Pfenniger, W. (1961). *Transition in the inlet length of tubes at high Reynolds numbers. In Boundary Layer and Flow Control.* (G. V. Lanchman, Ed.). Pergamon.

Reynolds, O. (1883). An Experimental Investigation of the Circumstances Which Determine Whether the Motion of Water Shall Be Direct or Sinuous, and of the Law of Resistance in Parallel Channels. *Philosophical Transactions of the Royal Society of London*, *174*(0), 935–982. https://doi.org/10.1098/rstl.1883.0029

Roach, P. E. and Brierley, D. H. (1992). The influence of a turbulent free-stream on zero pressure gradient transitional boundary layer development part I: test cases T3A and T3B. *Numerical Simulation of Unsteady Flows and Transition to Turbulence,* 319–347.

Rotta, J. (1956). An Experimental Contribution

to the Transition from Laminar to Turbulent flow in a Pipe. In *Proc., Int. Congress of Applied Mechanics*. (Vol. 3, pp. 350-359).

Saric, W. S., Reed, H. L., & Kerschen, E. J. (2002). Boundary-layer receptivity to STREAM DISTURBANCES. *Annu. Rev. Fluid Mech.*, *34*(1), 291–319. https://doi.org/10.1146/annurev.fluid.34.082701.161921

Schmid, P. J. (2001). *Stability and transition in shear flows*. (D. S. Henningson, Ed.). New York : New York .

Schubauer,. G. B. & Skramstad, H. K. (1948). Laminar boundary layer oscillations and transition on a flat plate. *NACA Rep. 909*.

Seddighi, M., He, S., Vardy, A. E., & Orlandi, P. (2014). Direct numerical simulation of an accelerating channel flow. *Flow, Turbulence and Combustion*, *92*(1–2), 473–502. https://doi.org/10.1007/s10494-013-9519-z

Tollmien, W. (1929). *Uber die entstehung der turbulenz. Nachr. Ges. Wiss. G¨ottingen 21-24 (English version: Tollmien, W.: The production of turbulence. NACA-TM-609-translated by D. M. Miner, Washington,D. C. 1931) translation.*

Van der Sande, E. (1980). Velocity Profiles in Accelerating Pipe Flows Starting from Rest. In *Proc. 3rd Int. Conf. on Pressure Surges* (p. pp 1-14). Canterburry, England.

Watmuff, J. H. (2004). Evolution of a Turbulent Wedge from a Streamwise Streak. In *15th Australasian Fluid Mechanics Conference* (pp. 13–17).

Wygnanski, I., Sokolov, M., & Friedman, D. (1975). On transition in a pipe. Part 2. The equilibrium puff. *J. Fluid Mech.*, *69*(2), 283–304. https://doi.org/10.1017/S0022112075001449

Zaki, T. A., & Saha, S. (2009). On shear sheltering and the structure of vortical modes in single- and two-fluid boundary layers. *Journal of Fluid Mechanics*, *626*, 111–147. https://doi.org/10.1017/S0022112008005648